JOURNAL OF SOLID STATE CHEMISTRY 94, 274–280 (1991)

A Mixed Valence Vanadium Phosphate with a Tunnel Structure: $Rb_6V_6P_6O_{31}$

L. BENHAMADA, A. GRANDIN, M. M. BOREL, A. LECLAIRE, AND B. RAVEAU

Laboratoire CRISMAT-ISMRA, Boulevard du Maréchal Juin 14050 Caen cédex, France

Received January 17, 1991; in revised form April 23, 1991

A new mixed-valence vanadium phosphate $Rb_6V_6P_6O_{31}$ has been isolated. Its structure was determined from single-crystal X-ray diffraction data. It crystallizes in the orthorhombic space group *Pnma* with $a = 7.0656(4)$ Å, $b = 13.4988(8)$ Å, $c = 14.4198(9)$ Å, $v = 1375.3(2)$ Å^3, $Z = 4$, $R = 0.049$, and $R_w = 0.052$ for 1058 unique reflections with $I > 3\sigma(I)$. The three-dimensional framework $[V_6P_6O_{31}]_\infty$ can be described by the assemblage of octahedral $[VO_3]_\infty$ chains with double chains $[V_2P_2O_{10}]_\infty$ built up from single PO_4 tetrahedra and double pyramidal units V_2O_9. The cohesion of the framework is achieved by P_2O_7 groups which share their corners with V_2O_9 units. This host lattice delimits very large tunnels running along **b** and five-sided tunnels running along **a**. The rubidium cations are located at the intersection of these tunnels.

Introduction

The studies of the catalytic properties of vanadium phosphorus oxides by Bordes and Courtine (*1*) have shown that these materials can act as heterogeneous catalysts in oxidation of hydrocarbons. Among the different vanadium phosphates, those which are the best known for their catalytic properties belong to the V–P–O system, and correspond to a molar ratio P : V = 1, as shown for instance for $V_2P_2O_9$ (*2*) and VPO_5 (*1, 3, 4*). Moreover it seems that oxidation states of vanadium ranging from IV to V should be of great importance for the existence of such properties. The recent studies of the K–V–P–O system have revealed its great ability to form vanadium phosphates with oxidation states smaller than V as shown for the compounds $KVPO_5$ (*5*), $K_2VP_2O_8$ (*6*), $K_2V_3P_4O_{17}$ (*7–9*), $K_6V_2P_4O_{16}$ (*10*), and KVP_2O_7 (*11, 12*). The chemistry of vanadium phosphates containing other alkali metal cations is also promising as shown for lithium, rubidium, and cesium phosphates (*6–9, 11–13*). From the oxidation catalysis point of view it appears that vanadium phosphates characterized by a mixed valence V (IV)/V(V) should be investigated. However, a very limited number of such mixed valence phosphates—$RbV_3P_4O_{17+x}$ (*14*) and $KV_3P_4O_{16}$ (*15*)—have been reported up to now. The present paper deals with the synthesis and crystal structure of a new mixed valent rubidium phosphate $Rb_6V_6P_6O_{31}$.

Synthesis

The synthesis of $Rb_6V_6P_6O_{31}$ was performed in two steps. First, an adequate mixture of Rb_2CO_3, $H(NH_4)_2PO_4$, and V_2O_5 were heated up to 673 K in air in order to

0022-4596/91 $3.00

TABLE I

$Rb_6V_6P_6O_{31}$: INTERETICULAR DISTANCES

h	k	l	d_{obs} (Å)	d_{calc} (Å)	I
0	1	3	4.539	4.528	19
1	2	2	4.049	4.042	23
1	3	1	3.677	3.670	31
2	0	1	3.434	3.431	82
0	4	0	3.371	3.374	33
2	1	1	3.321	3.326	20
1	0	4	3.213	3.211	48
0	2	4	3.186	3.180	96
2	2	0	3.136	3.130	34
2	1	2	3.093	3.088	34
2	2	1	3.064	3.059	71
1	4	1	2.984	2.979	100
2	2	2	2.877	2.871	26
2	0	3	2.855	2.847	23
1	4	2	2.810	2.805	53
2	3	1	2.723	2.728	17
1	0	5	2.674	2.670	35
2	3	2	2.594	2.593	23
1	4	3	2.576	2.572	14
2	0	4	2.526	2.523	17
1	5	1	2.487	2.484	14
0	4	4	2.467	2.464	16
0	3	5	2.432	2.428	14
2	4	1		2.428	
2	3	3	2.407	2.406	21
1	3	5	2.295	2.296	15
3	0	2	2.238	2.238	15
3	1	2	2.207	2.209	20
2	4	3	2.179	2.176	12
0	6	2	2.149	2.148	13
3	2	2	2.124	2.124	24
1	4	5	2.093	2.094	13
2	5	2	2.058	2.056	11
2	4	4	2.023	2.021	17
3	0	4	1.973	1.972	13
2	5	3	1.960	1.959	11
1	1	7	1.957	1.957	36
0	7	1	1.912	1.911	22
3	4	2	1.865	1.866	27

eliminate CO_2, H_2O, and NH_3. In the second step the finely ground product was mixed with an appropriate amount of vanadium and sealed in an evacuated silica ampoule. This sample was then heated up at 870 K for 2 months.

Single crystals of this phase were grown from a sample of nominal composition "$RbVPO_5$." The method of preparation was identical to that described above for the quantitative synthesis of the powder.

The powder X-ray diffraction pattern of this phase was indexed in an orthorhombic cell (Table I) in agreement with the parameters obtained from the single crystal study (Table II).

Structure Determination

A mauve crystal with dimensions 0.154 × 0.038 × 0.026 mm was selected for the structure determination. The cell parameters reported in Table II were determined and refined by diffractometric techniques at 294 K with a least squares refinement based upon 25 reflections with $36° < \theta < 44°$.

The data were collected on a CAD-4 Enraf-Nonius diffractometer with the data collection parameters reported in Table II. The

TABLE II

SUMMARY OF CRYSTAL DATA, INTENSITY MEASUREMENTS, AND STRUCTURE REFINEMENT PARAMETERS FOR $Rb_6V_6P_6O_{31}$

1. Crystal data	
Space group	*Pnma*
Cell dimensions	a = 7.0656(4) Å
	b = 13.4988(8)
	c = 14.4198(9)
Volume	1375.3(2) Å^3
Z	4
2. Intensity measurements	
λ (Cu$K\alpha$)	1.54056 Å
Scan mode	$\omega - \frac{2}{3}\theta$
Scan width	1 + 0.14 tg θ
Slit aperture (mm)	1 + tg θ
Max θ (°)	78
Reflection with $I > 3\sigma$	1058
Standard reflections	3 measured every 3000 sec
μ	34.4 mm^{-1}
3. Structure solution and refinement	
Parameters refined	130
Agreement factors	R = 0.049
	R_w = 0.052
Weighting scheme	$W = f(\sin\theta/\lambda)$
Δ/σ_{max}	0.05

TABLE III

POSITIONAL PARAMETERS AND THEIR ESTIMATED STANDARD DEVIATIONS

Atom	x	y	z	B(Å^2)
Rb(1)	0.0962(1)	0.00833(8)	0.16277(6)	1.89(1)
Rb(2)	0.1080(2)	0.250	−0.00604(9)	1.56(2)
V(1)	0.1492(2)	0.1246(1)	0.4231(1)	0.81(2)
V(2)	0.2598(3)	0.750	0.2401(1)	0.42(3)
P(1)	0.0421(3)	0.8999(2)	0.3809(1)	0.55(3)
P(2*a*)[a]	0.3523(8)	0.250	0.2603(4)	0.89(9)
P(2*b*)[a]	0.2637(8)	0.250	0.2402(4)	0.89(9)
O(1)	0.3235(9)	0.0684(6)	0.4716(4)	1.5(1)
O(2)	0.205(1)	0.250	0.4560(6)	1.3(2)
O(3)	0.0275(8)	0.0124(5)	0.3586(4)	1.0(1)
O(4)	−0.0551(8)	0.1170(5)	0.5138(4)	0.97(9)
O(5)	0.2645(9)	0.1569(5)	0.2972(5)	1.3(1)
O(6)	0.045(1)	0.750	0.2000(6)	0.9(1)
O(7)	0.3646(8)	0.6477(5)	0.1590(4)	0.99(9)
O(8)	0.2219(8)	0.6432(5)	0.3364(4)	0.92(9)
O(9)	0.390(2)	0.250	0.1582(7)	2.6(2)
O(10)[a]	0.058(3)	0.250	0.190(2)	2.6(5)

Note. Anisotropically refined atoms are given in the form of the isotropic equivalent displacement parameter defined as

$$B = \frac{4}{3}\sum_i\sum_j \mathbf{a}_i \cdot \mathbf{a}_j \cdot \beta_{ij}.$$

[a] Half-occupied site.

reflections were corrected for Lorentz and polarization effects; no absorption corrections were performed.

Atomic coordinates of the vanadium atom were deduced from the Patterson function and the other atoms located by subsequent Fourier series.

The difference synthesis revealed that one of the phosphorus atoms, P(2), is statistically distributed over two splitted positions (P(2*a*) and P(2*b*)), which are only half occupied owing to their short distance. This feature will be discussed later.

Refinement of the atomic coordinates and their anisotropic thermal parameters led to $R = 0.049$ and $R_w = 0.052$ and to atomic parameters of Table III.

Description of the Structure and Discussion

The projection of the structure of this new phase onto the (100) plane (Fig. 1) shows that its host lattice $[V_6P_6O_{31}]_\infty$ consists of corner-sharing VO_5 pyramids (labeled V(1)), VO_6 octahedra (labeled V(2)), and PO_4 tetrahedra (labeled P(1) and P(2), respectively).

The geometry of the P(1) tetrahedra is characteristic of that observed in mono-

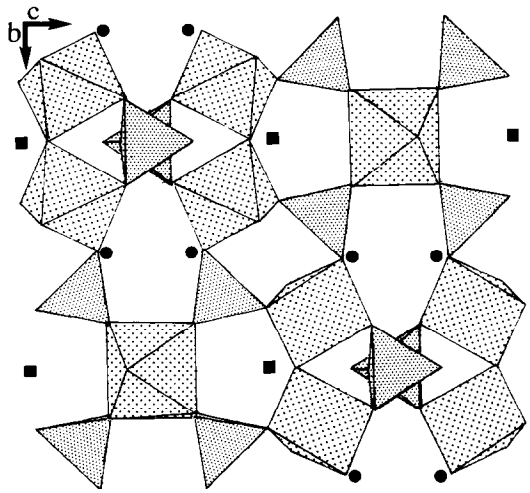

FIG. 1. Projection of the structure along **a**.

TABLE IV

DISTANCES (Å) AND ANGLES (°) IN THE PO_4 TETRAHEDRA

P(1)	O(3^{iii})	O(4^{iv})	O(7^{v})	O(8^{ii})
O(3^{iii})	1.556(7)	2.545(9)	2.462(9)	2.529(9)
O(4^{iv})	110.6(4)	1.539(6)	2.523(9)	2.486(9)
O(7^{v})	106.2(4)	111.0(4)	1.522(6)	2.526(8)
O(8i^{ii})	109.7(4)	107.8(4)	111.3(4)	1.537(6)
P(2a)	O(5)	O(5^{vi})	O(9)	O(10^{vii})
O(5)	1.500(8)	2.51(2)	2.53(1)	2.43(2)
O(5^{vi})	113.9(7)	1.500(8)	2.53(1)	2.43(2)
O(9)	115.0(5)	115.0(5)	1.497(12)	2.49(1)
O(10^{vii})	102.3(6)	102.3(6)	105.9(8)	1.61(2)
P(2b)	O(5)	O(5^{vi})	O(9)	O(10)
O(5)	1.502(9)	2.51(2)	2.53(1)	2.47(1)
O(5^{vi})	113.6(8)	1.502(9)	2.53(1)	2.47(1)
O(9)	115.7(5)	115.7(5)	1.48(1)	2.399(2)
O(10)	104.2(6)	104.2(6)	100.7(9)	1.63(2)

Note. The diagonal terms are the P–O(i) distances, the terms above the diagonal are the O(i)–O(j) distances, and those below are the O(i)–P–O(j) angles.

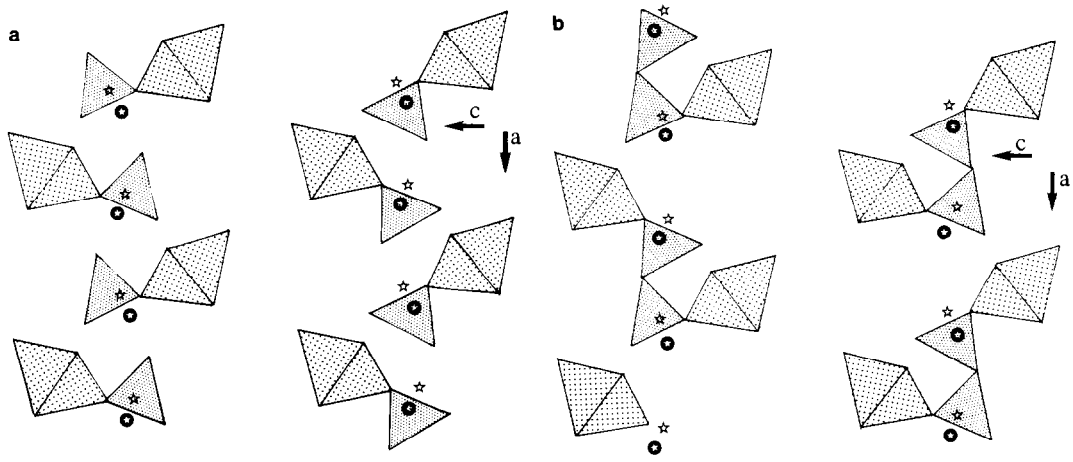

FIG. 2. The two hypotheses of the arrangement of P(2) tetrahedra in the structure: (a) rows of PO_4: ☆, P(2a) ✪, P(2b); (b) rows of P_2O_7: ☆, P(2a) ✪, P(2b).

phosphates. Each P(1) tetrahedron indeed shares its corners with two VO_5 pyramids and two VO_6 octahedra; consequently, the P–O distances in these monophosphate groups are almost equal (Table IV). Considering the P(2) tetrahedra, two hypothesis can be proposed for their arrangement in the structure:

(i) P(2) tetrahedra form rows of monophosphate groups, PO_4, running along **a**. Two sites (2(*a*) and 2(*b*) are possible for P in each row (Fig. 2a)); when one site is occupied, the adjacent one must be empty in the same row so that for one row, only one type of site can be occupied by phosphorus (2(*a*) or 2(*b*)). On the contrary, for two neigh-

TABLE V

DISTANCES (Å) AND ANGLES (°) IN THE VO_5 SQUARE PYRAMID AND THE VO_6 OCTAHEDRON

V(1)	O(1)	O(2)	O(3)	O(4)	O(5)
O(1)	1.607(7)	2.602(9)	2.757(9)	2.821(9)	2.81(1)
O(2)	99.4(4)	1.801(4)	3.72(1)	2.699(9)	2.65(1)
O(3)	100.2(4)	160.0(4)	1.974(7)	2.710(9)	2.72(1)
O(4)	104.5(3)	91.9(4)	87.34(3)	1.951(6)	3.89(1)
O(5)	100.5(3)	87.0(4)	85.33(3)	154.8(4)	2.036(7)

V(2)	O(6)	O(6^{i})	O(7)	O(7^{ii})	O(8)	O(8^{ii})
O(6)	1.624(9)	3.82(1)	2.71(1)	2.71(1)	2.74(1)	2.74(1)
O(6^{i})	177.7(3)	2.193(9)	2.77(1)	2.77(1)	2.75(1)	2.75(1)
O(7)	98.1(3)	83.5(3)	1.956(7)	2.76(1)	2.75(1)	3.94(1)
O(7^{ii})	98.1(3)	83.5(3)	89.8(4)	1.956(7)	3.94(1)	2.75(1)
O(8)	96.9(3)	81.4(3)	87.5(3)	164.9(3)	2.020(7)	2.88(1)
O(8^{ii})	96.9(3)	81.4(3)	164.9(3)	87.5(3)	91.1(4)	2.020(7)

Note. The diagonal terms are the V–O(i) distances, the terms above the diagonal are the O(i)–O(j) distances, and those below are the O(i)–V–O(j) angles.

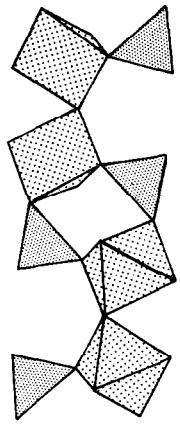

FIG. 3. The $(V_2P_2O_{10})_\infty$ chains along **b**.

boring rows the P sites are not correlated, i.e., one can observe 2(*a*)–2(*a*) or 2(*b*)–2(*b*) or 2(*a*)–2(*b*) occupancy. Thus the PO_4 tetrahedra obey only the **a** translation but not **b** and **c** translations. The computed crystal, the structure of which is in fact the average of all the cells of the real crystal, shows a splitting of P(2) over two sites, *a* and *b*. This average is not a dynamic one, the phosphorus does not jump from 2*a* to 2*b*, it is a "static average." In this hypothesis such tetrahedra would have two free apices and the resulting formula should be $Rb_6V_6P_6O_{32}$.

(ii) P(2) tetrahedra consist of rows of diphosphate groups P_2O_7, running along **a** showing a "static average" similar to that described above (Fig. 2b). In this case each tetrahedron would only have one free apex, and the O(10) oxygen site is half occupied; this leads to the formula $Rb_6V_6P_6O_{31}$.

The examination of the P(2)–O distances (Table IV) shows that there exists one short P–O distance, two intermediate P–O distances, and one long P–O bond per tetrahedron. Consequently, it strongly supports the second hypothesis, since the shorter and longer P–O bonds correspond to the free and bridging oxygen atoms, respectively, and the bridging angle P–O–P = 127°. The existence of P_2O_7 groups is also supported by the fact that they ensure the cohesion of the framework and the *R* factor is lowered from 0.052 to 0.049.

The pyramidal coordination of V(1) is characteristic of the vanadyl group, as shown from the existence of the abnormally short apical V–O bond (Table V) which cor-

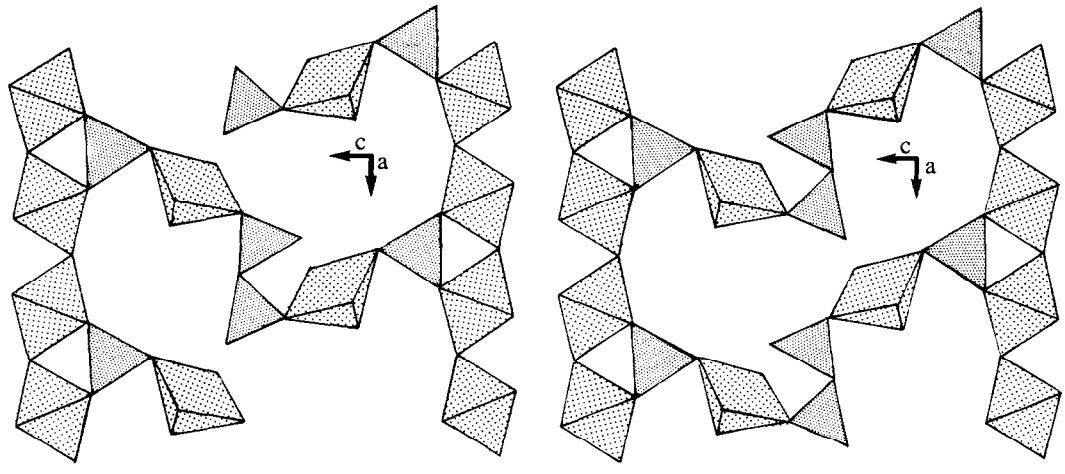

FIG. 4. The two arrangements of P_2O_7 groups in the structure.

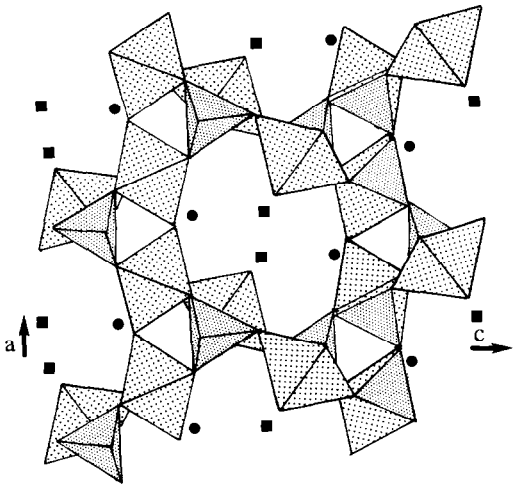

FIG. 5. Projection of the structure along **b**.

responds to the free oxygen atom of the VO_5 pyramid.

Although located in an almost regular "O_6" octahedron, the V(2) atom exhibits one very short V–O bond, of 1.624 Å, similar to that observed in vanadyl ions and directed along **a**, whereas the longest bond (2.193 Å) appears in the opposite direction. Such behavior has already been described in $V_2P_2O_9$ (2).

The analysis of the three-dimensional framework allows the following features to be shown:

(i) The framework is built up from ReO_3-type chains $[VO_3]_\infty$ (Fig. 1) of corner-sharing octahedra running along **a**.

(ii) The VO_5 pyramids form $[V_2O_9]$ units of two corner-sharing VO_5 pyramids.

(iii) The V_2O_9 units and the single PO_4 tetrahedra share their corners forming double $[V_2P_2O_{10}]_\infty$ chains running along **b** (Fig. 3).

(iv) The P_2O_7 groups ensure the connection between two V_2O_9 units (Fig. 4) by sharing four of their apices with two V_2O_9 units, whereas the two remaining corners are free. In fact two localizations of the P_2O_7 groups are possible (Figs. 4a and 4b) without changing the framework $[V_6P_6O_{31}]_\infty$.

Thus the host lattice $[V_6P_6O_{31}]_\infty$ can be described by the assemblage of the octahedral $[VO_3]_\infty$ chains with the $[VPO_5]_\infty$ chains (Fig. 1); in this framework the $[VO_3]_\infty$ chains share the corners of their octahedra with the corners of the PO_4 tetrahedra of the $[V_2P_2O_{10}]_\infty$ chains. The cohesion of the structure is achieved by the P_2O_7 groups which share their corners with the V_2O_9 units (Fig. 4).

The view of the structure along **a** (Fig. 1) shows that this framework delimits five-sided tunnels running along **a** similar to those observed in diphosphate tungsten bronzes $P_2O_4(WO_3)_{2m}$ (*16*) and in $Na_4Nb_8P_4O_{35}$ (*17*); similar rings are also observed in $K_2V_3P_4O_{17}$ (*8*). However, the five-sided rings of $Rb_6V_6P_6O_{31}$ differ from the other phosphates, by the fact that two NbO_6 or WO_6 octahedra are replaced by two VO_5 pyramids.

Another original feature of this structure deals with the existence of very large tunnels (Fig. 5) running along **b**, so that this

TABLE VI

SURROUNDING OF Rb^+ WITH Rb–O < 3.40 Å

Rb(1)–O(1^{ix})	2.998(7)	Rb(2)–O(1)	3.209(8)
Rb(1)–O(1^{viii})	2.851(7)	Rb(2)–O(1^{viii})	3.209(8)
Rb(1)–O(3)	2.866(6)	Rb(2)–O(2^{xii})	2.940(9)
Rb(1)–O(3^{x})	3.064(6)	Rb(2)–O(4^{vii})	2.984(7)
Rb(1)–O(5)	3.032(7)	Rb(2)–O(4^{x})	2.984(7)
Rb(1)–O(5^{viii})	3.138(7)	Rb(2)–O(6^{xiii})	2.998(10)
Rb(1)–O(7^{vi})	2.835(7)	Rb(2)–O(8^{xv})	2.948(7)
Rb(1)–O(8^{xi})	3.343(6)	Rb(2)–O(8^{xiv})	2.948(7)
Rb(1)–O(8^{vi})	3.352(6)	Rb(2)–O(9)	3.097(11)
Rb(1)–O(10)	3.297(2)	Rb(2)–O(10)	2.850(14)

Note. Symmetry codes: (i) $\frac{1}{2} + x, \frac{3}{2} - y, \frac{1}{2} - z$; (ii) $x, \frac{3}{2} - y, z$; (iii) $x, y + 1, z$; (iv) $-x, 1 - y, 1 - z$; (v) $-\frac{1}{2} + x, \frac{3}{2} - y, \frac{1}{2} - z$; (vi) $x, \frac{1}{2} - y, z$; (vii) $\frac{1}{2} + x, \frac{1}{2} - y, \frac{1}{2} - z$; (viii) $-\frac{1}{2} + x, y, \frac{1}{2} - z$; (ix) $\frac{1}{2} - x, -y, -\frac{1}{2} + z$; (x) $\frac{1}{2} + x, y, \frac{1}{2} - z$; (xi) $-\frac{1}{2} + x, \frac{1}{2} - y, \frac{1}{2} - z$; (xii) $-\frac{1}{2} + x, \frac{1}{2} - y, z$; (xiii) $-x, -\frac{1}{2} + y, -z$; (xiv) $\frac{1}{2} - x, 1 - y, \frac{1}{2} - z$; (xv) $\frac{1}{2} - x, -\frac{1}{2} + y, -\frac{1}{2} + z$.

oxide can also be described as an intersecting tunnel structure. The rubidium cations are located in these large tunnels at the intersection with pentagonal tunnels, with Rb–O distances ranging from 2.83 to 3.35 Å (Table VI).

This structural study suggests for this compound a possibility of nonstoichiometry on rubidium, but also of ion-exchange properties owing to the large size of the tunnels.

The valence of vanadium in the two sorts of sites, pyramidal and octahedral, should also be investigated.

References

1. E. Bordes and P. Courtine, *J. Chem. Soc. Chem. Commun.* **47,** 294 (1985).
2. N. Middlemiss, Ph.D. thesis, MacMaster Univ, Canada.
3. B. Jordan and C. Calvo, *Canad. J. Chem.* **51,** 2621 (1973).
4. E. Bordes and P. Courtine, *J. Chem. Soc. Chem. Commun.* **47,** 291 (1985).
5. L. Benhamada, A. Grandin, M. M. Borel, A. Leclaire, and B. Raveau, *Acta Crystallogr.*, **C47,** 1138 (1991).
6. Yu E. Gorbunova, S. A. Linde, A. K. Lavrow, and I. V. Tananaev, *Dokl. Akad. Nauk. SSSR* **250**(2), 350 (1980).
7. A. Leclaire, H. Chahboun, D. Groult, and B. Raveau, *J. Solid State Chem.* **27,** 170 (1988).
8. K. H. Lii, H. J. Tsai, and S. L. Wang, *J. Solid State Chem.* **87,** 396 (1990).
9. K. H. Lii, Y. P. Wang, C. Y. Cheng, S. L. Wang, and H. C. J. Chin, *Chem. Soc. (Taipi)* **37,** 141 (1990).
10. L. Benhamada, A. Grandin, M. M. Borel, and B. Raveau. *J. Solid State Chem.*, **91,** 264 (1991).
11. A. V. Lavrow, M. Ya Voitenkov and E. G. Tselebrouskaya, *Inorg. Mater.* **17,** 73 (1981).
12. L. Benhamada, A. Grandin, M. M. Borel, A. Leclaire and B. Raveau, *Acta Crystallogr.*, **C47,** 424 (1991).
13. Y. P. Wang and K. H. Lii, *Acta Crystallogr. Sect. C* **45,** 1210 (1989).
14. K. H. Lii and C. S. Lee, *Inorg. Chem.* **29,** 3298 (1990).
15. C. S. Lee and K. H. Lii *J. Solid State Chem.* **92,** 362 (1991).
16. M. Hervieu, B. Domengés, and B. Raveau, *J. Solid State Chem.* **58,** 223 (1985).
17. A. Benabbas, M. M. Borel, A. Grandin, A. Leclaire, and B. Raveau. *J. Solid State Chem.* **89,** 75 (1990).